ACS OMEGA

Open Access

http://pubs.acs.org/journal/acsodf

Article

Rubbery Soft Polymer Electrolyte Membrane with a Nanomatrix Channel Prepared from Natural Rubber

Yoshimasa Yamamoto* and Seiichi Kawahara

Cite This: *ACS Omega* 2025, 10, 17576−17583

Read Online

ACCESS | Metrics & More | Article Recommendations | Supporting Information

ABSTRACT: Rubbery soft polymer electrolyte membranes (PEMs) prepared from naturally occurring products are in high demand for the fabrication of flexible fuel cells as a multipurpose energy source to achieve a carbon-neutral society. This work describes the preparation of a rubbery soft PEM from deproteinized natural rubber (DPNR) by grafting-copolymerizing ethyl *p*-styrenesulfonate (SSEt) onto the surface of rubber particles in the latex stage, followed by hydrolysis with NaOH and cast film formation to construct a nanomatrix channel. The resulting rubbery soft PEM, a graft copolymer of DPNR and poly(*p*-styrenesulfonic acid) (DPNR-*graft*-PSS), is characterized by ^{1}H NMR spectroscopy, transmission electron microscopy (TEM), impedance analysis, and tensile testing. The hydrophobic rubber particles with a diameter of about 1 μm are well dispersed in the continuous nanochannel of hydrophilic poly(*p*-styrenesulfonic acid) with a thickness of about 10 nm that possesses a high proton conductivity, owing to an efficient proton transportation, which is beneficial for polymer electrolyte fuel cells. σ^* is the proton conductivity per unit equivalent of sulfonic acid, which is distinguished from the proton conductivity, σ. The value of σ^* for the DPNR-*graft*-PSS prepared with 1.0 mol/kg-rubber of SSEt is 2.6 (S/cm)/meq, which is approximately 1.4 times higher than that of the perfluorosulfonic acid membrane Nafion117, whereas its σ is lower. The apparent activation energy of DPNR-*graft*-PSS (3.2 kJ/mol) is lower than that of Nafion117, and its stress at break (6.9 MPa) is higher than that of DPNR. The high σ^*, low apparent activation energy, and outstanding tensile strength of DPNR-*graft*-PSS can be attributed to the formation of the nanomatrix channel.

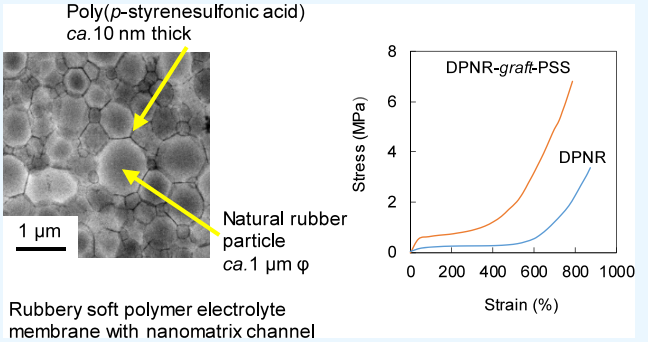

INTRODUCTION

Rubbery soft polymer electrolyte membranes (PEMs) with a nanomatrix channel prepared from natural rubber[1−3] are sustainable functional materials that can potentially achieve an efficient proton transportation, which is required for flexible polymer electrolyte fuel cells to generate green electrical energy. This nanomatrix channel is responsible for proton transportation owing to its nanophase-separated structure consisting of hydrophobic polymer particles with a diameter of approximately 1 μm covered with a continuous nanochannel of a hydrophilic functional polymer (Figure 1). As the hydrophobic polymer particles for the nanomatrix channel of rubbery soft PEMs, natural rubber, which is isolated from *Hevea brasiliensis* as a latex in which hydrophobic rubber particles with a diameter of approximately 1 μm are dispersed in water,[4,5] offers a sustainable green resource.

Meanwhile, the hydrophilic functional polymer as the nanochannel plays an important role in proton transportation in rubbery soft PEMs. Polymer electrolyte fuel cells generate electrical energy and water via an electrochemical reaction between hydrogen and oxygen,[6] for which protons must be transported from the anode to the cathode through the PEM. In PEMs, which are generally used under a high humidity

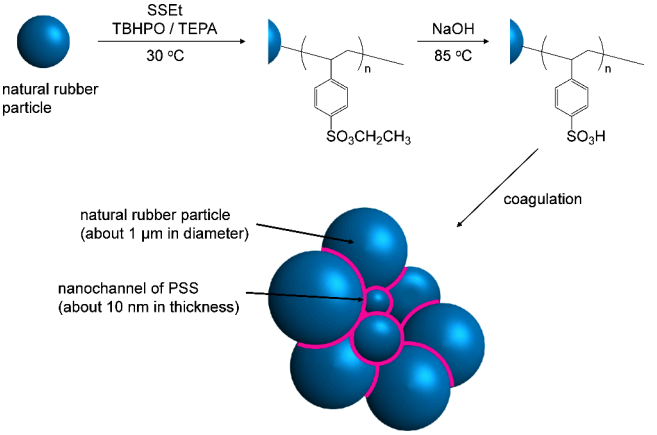

Figure 1. Strategy of the formation of the nanomatrix channel.

Received: December 17, 2024
Revised: February 18, 2025
Accepted: April 15, 2025
Published: April 23, 2025

condition, the protons are transported by connecting individual ion clusters with a diameter of approximately 5−10 nm through a channel with a thickness of several nanometers.[7,8] Thermal fluctuation may induce the connection and disconnection of these ion clusters, causing inhibition of the proton transportation.[9] Thus, an efficient proton transportation could be achieved by confining the ion clusters into a nanochannel with a thickness of about 10 nm to maintain the connection of the individual ion clusters without the influence of the thermal fluctuation.

The perfluorosulfonic acid polymer membrane Nafion117 is a PEM with outstanding proton conductivity and chemical stability, which render its widely used in applications including fuel cell vehicles and household power generators and so forth.[10] However, owing to the persistency of per- and polyfluotoalkyl substances in the environment,[11] PEMs based on hydrocarbons such as poly(styrenesulfonic acid),[12,13] poly(ether ether ketone),[14,15] polyphenylene,[16,17] poly(ether sulfone),[18,19] and sulfonated polyimide[20,21] have become an alternative research target. In particular, cross-linked poly(styrenesulfonic acid) (PSS) with a high density of sulfonic acid groups exhibits excellent proton conductivity.[22] Hillmyer and co-workers reported the preparation of a block copolymer consisting of polystyrene and PSS, in which the bicontinuous structure with a PSS domain size of approximately 10 nm contributed to achieving an excellent proton conductivity comparable to that of Nafion117.[23] Thus, together with natural rubber as the hydrophobic polymer particles, PSS could be used as a hydrophilic nanochannel to prepare rubbery soft PEMs with a nanomatrix channel.

In our previous studies, a natural rubber-*graft*-polystyrene copolymer was prepared via graft copolymerization of styrene onto the surface of natural rubber particles in the latex stage, with the molecular weight of the grafted polystyrene being approximately 10^4 g/mol.[2,24] Subsequently, a PEM with a nanomatrix channel was prepared by sulfonating the grafted polystyrene with chlorosulfonic acid. The resulting PEM accomplished a high proton conductivity of 0.095 S/cm, outperforming Nafion 117.[1−3] However, the PEM was too brittle for application in polymer electrolyte fuel cells because chlorosulfonic acid resulted in not only the sulfonation of grafted polystyrene but also the cyclization of natural rubber.[25,26] To avoid this cyclization, styrene substituted with a sulfonic acid precursor such as a sulfonic acid ester could be used for the graft copolymerization.

In this study, a rubbery soft PEM with a nanomatrix channel was prepared by grafting-copolymerizing ethyl *p*-styrenesulfonate (SSEt) onto the surface of natural rubber particles in the latex stage, followed by hydrolysis with NaOH and cast film formation. The resulting PEM was characterized by ^{1}H NMR spectroscopy, transmission electron microscopy (TEM), impedance analysis, and tensile testing.

EXPERIMENTAL SECTION

Materials. Natural rubber used in this study was commercial high ammonia natural rubber latex (HANR) with a dry rubber content (DRC) of approximately 60 w/w%. Sodium dodecyl sulfate (SDS), *tert*-butylhydroperoxide (TBHPO), and tetraethylenepentamine (TEPA) were purchased from Kishida Chemical Co., Ltd. Sodium *p*-styrenesulfonate (SSNa) and bromoethane were obtained from Tokyo Chemical Industry Co., Ltd. Urea, silver nitrate, acetonitrile, hexane, ethyl acetate, sodium hydroxide, hydrochloric acid, and sodium hypochlorite were purchased from Nakalai Tesque, Inc. Acetone-d_6, DMSO-d_6, and chloroform-*d* were provided by Kanto Chemical Co., Inc. Nafion117 and ruthenium chloride were purchased from Sigma-Aldrich Co.

Preparation of Deproteinized Natural Rubber (DPNR) Latex. Deproteinization of the HANR latex was performed by incubating the latex with 0.1 w/w% urea in the presence of 1 w/w% SDS at room temperature for 1 h, followed by centrifugation at 10,000 × *g*. The resulting cream fraction was redispersed in a 0.5 w/w% SDS solution to produce 30 w/w% DRC latex, which was washed twice by centrifugation to obtain the DPNR latex. The DRC of the DPNR latex was adjusted to 30 w/w% with a 0.1 w/w% SDS solution.

Preparation of Ethyl *p*-Styrenesulfonate (SSEt).[27] SSNa (113 g, 0.55 mol) was dissolved in 500 mL of H_2O, and then, a 1 mol/L $AgNO_3$ (85 g, 0.50 mol) aqueous solution was added into the solution at 0 °C. After stirring at 0 °C for 2 h in the dark, the reaction mixture was filtered and washed with H_2O. The crude product was dissolved in 1 L of CH_3CN. After filtration of the solution, the filtrate was evaporated to obtain silver *p*-styrenesulfonate in 79% yield.

The as-obtained silver *p*-styrenesulfonate (29 g, 0.10 mol) was converted into SSEt by stirring with bromoethane (16 g, 0.11 mol) in 400 mL of CH_3CN at 70 °C for 12 h. After the reaction mixture was filtered, the filtrate was evaporated. The crude product was purified by silica gel column chromatography using ethyl acetate−hexane (1:1) as the eluent to obtain SSEt in 73% yield.

Graft Copolymerization of SSEt. The graft copolymerization of SSEt was performed using TBHPO−TEPA as an initiator. The DPNR latex was charged with N_2 gas for 3 h at 30 °C, followed by the successive addition of the initiator and the monomer. The reaction was conducted by stirring the latex at approximately 300 rpm for 3 h at 30 °C. A film of the graft copolymer of DPNR and poly(ethyl *p*-styrenesulfonate) (DPNR-*graft*-PSSEt) was prepared by casting the gross polymer latex into a Petri dish and drying under reduced pressure at 50 °C. The PSSEt homopolymer was removed from the gross polymer by extracting with a 3:1 acetone−2-butanone mixture in a Soxhlet apparatus under a N_2 atmosphere in the dark.

Hydrolysis of DPNR-*graft*-PSSEt. The DPNR-*graft*-PSSEt latex and SDS were added to a 0.1 mol/L NaOH solution to obtain a solution with 2 w/w% DRC and 0.1 w/w% SDS. After stirring at 85 °C for 3 h and subsequent neutralization with 1 mol/L HCl solution, a film of the graft copolymer of DPNR and PSS (DPNR-*graft*-PSS) was prepared by casting the gross polymer latex into a Petri dish and drying under reduced pressure at 50 °C. The PSS homopolymer was removed from the gross polymer by immersing the as-cast film in a 1 mol/L HCl solution for 24 h followed by drying under reduced pressure at 50 °C.

Characterization. NMR measurements were performed by using a JEOL ECX-400 spectrometer. For the solution-state ^{1}H NMR measurement of DPNR, SSEt, and PSSEt, the specimen was dissolved in $CDCl_3$ or acetone-d_6. The chemical shifts are referenced to tetramethylsilane. For the rubber-state ^{1}H NMR measurement of the graft copolymer, the specimen was swelled with acetone-d_6 or DMSO-d_6 for 3 days in a sample tube with an outer diameter of 3.2 mm and analyzed using a field-gradient magic angle spinning probe with a pulse repetition time of 7 s and a spinning rate of 8 kHz.

https://doi.org/10.1021/acsomega.4c11363
ACS Omega 2025, 10, 17576−17583

The ion exchange capacity (IEC) of the samples was measured by using the titration method. Before the IEC measurement, the sample was immersed in a 1 mol/L HCl solution for 24 h, washed with H_2O, and dried under reduced pressure at 50 °C. The resulting sample was immersed in a sat. NaCl for 24 h to replace H^+ with Na^+. The H^+ in the solution was titrated with a 0.01 mol/L NaOH solution in the presence of phenolphthalein as an indicator. The IEC was calculated using the following equation:

$$\mathrm{IEC(meq/g)} = \frac{C_{\mathrm{NaOH}} \times V_{\mathrm{NaOH}}}{W} \quad (1)$$

where C_{NaOH}, V_{NaOH}, and W are the concentration of NaOH (mol/L), the volume of NaOH solution consumed in the titration (mL), and the weight of the sample (g), respectively.

The proton conductivity was measured with a Solartron SI 1260 impedance/gain-phase analyzer in a frequency range between 10^{-3} and 10^{6} Hz at an AC voltage amplitude of 50 mV. The impedance was measured by placing the cell in a temperature- and humidity-controlled chamber (ESPEC SH-221) with a temperature ranging from 40 to 80 °C and a relative humidity of 100%. Before the measurement, the membrane was immersed in a 1 mol/L HCl solution for 24 h, washed with H_2O, and dried under reduced pressure at 50 °C. The resulting membrane was hydrated by immersion in H_2O for 1 h. The conductivity (σ) of the membrane was calculated using the following equation:

$$\sigma\mathrm{(S/cm)} = \frac{d}{RA} \quad (2)$$

where d, R, and A are the thickness of the sample (cm), the membrane resistance (Ω), and the surface area of the membrane (cm^2), respectively.

The morphology of DPNR-*graft*-PSS was observed via TEM using a JEOL JEM-2100 microscope at an accelerating voltage of 200 kV. The ultrathin section for the TEM observation was prepared using a microtome (Ultracut N, Reichert-Nissei FC S) at −75 °C, followed by staining with RuO_4 vapor generated from ruthenium chloride and sodium hypochlorite at room temperature for 1 min.

The tensile test was performed at room temperature using an Instron universal tensile tester (Instron model 3365) according to JIS K6251. The film samples were cut with dumbbell-shaped type 7. The test piece was stretched at a speed of 200 mm/min. The tensile test was repeated three times for each specimen, and the averages of the three curves are given as the results.

RESULTS AND DISCUSSION

Graft Copolymerization of SSEt. The hydrophobic monomer SSEt was used for the graft copolymerization instead of the hydrophilic *p*-styrenesulfonic acid because the latter was homopolymerized in the serum of the latex, preventing the graft copolymerization onto natural rubber particles (see the Supporting Information). Furthermore, DPNR latex was used for the graft copolymerization of SSEt to avoid side reactions caused by the proteins present on the surface of the natural rubber particles in the latex stage.[28] Figure 1 shows the strategy adopted for the formation of a nanomatrix channel consisting of natural rubber particles and PSS.

Figure 2 shows solution-state ^{1}H NMR spectra for DPNR, SSEt and PSSEt and rubber-state ^{1}H NMR spectra after swelling with acetone-d_6 for DPNR-*graft*-PSSEt prepared with SSEt of 1.0 mol/kg-rubber and initiator of 2.0×10^{-2} mol/kg-rubber and acetone-extracted DPNR-*graft*-PSSEt. In the spectrum of DPNR, the signals characteristic of the methyl, methylene, and unsaturated methine protons of the *cis*-1,4-isoprene units appeared at 1.8, 2.1, and 5.1 ppm, respectively (Figure 2a). Meanwhile, in the spectrum of SSEt (Figure 2b), sharp signals appeared at 1.2, 4.1, 5.4, 6.0, 6.8, 7.7, and 7.8 ppm, among which the signals at 7.7 and 7.8 ppm were assigned to the phenyl group, those at 5.4, 6.0, and 6.8 ppm were assigned to the vinyl group, and those at 4.1 and 1.2 ppm were assigned to the ethyl group of ethyl sulfonate. After the homopolymerization of SSEt, broad signals attributable to the methylene group of the ethyl ester and the phenyl group of PSSEt appeared at 4.1 and 6.6−7.8 ppm, respectively, whereas the sharp signals characteristic of SSEt disappeared (Figure 2c). When SSEt was graft-copolymerized onto the natural rubber particles, broad signals characteristic of PSSEt appeared at 4.1 and 6.6−7.8 ppm in addition to the signals characteristic of the *cis*-1,4-isoprene units at 1.8, 2.1, and 5.1 ppm and very small signals of SSEt at 5.4 and 6.0 ppm (Figure 2d). After acetone extraction, these small signals disappeared, and the signals characteristic of PSSEt appeared (Figure 2e). These results confirm that the graft copolymerization of SSEt onto natural rubber particles proceeded in the latex stage with high conversion and grafting efficiency.

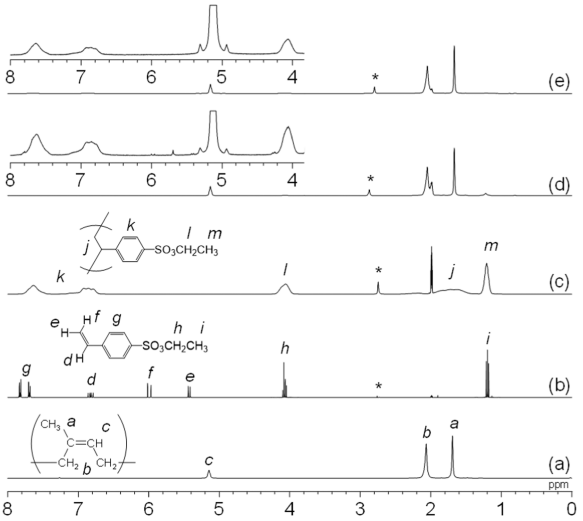

Figure 2. ^{1}H NMR spectra of (a) DPNR, (b) SSEt, (c) PSSEt, (d) DPNR-*graft*-PSSEt, and (e) acetone-extracted DPNR-*graft*-PSSEt. *H_2O in acetone-d_6.

From the intensity of the signals in the ^{1}H NMR spectra, the conversion and grafting efficiency of SSEt are calculated using the following eqs 3 and 4, respectively:

$$\mathrm{conversion(\%)} = \frac{I_{6.6-7.8} - I_{6.0} \times 5}{I_{6.6-7.8}} \times 100 \quad (3)$$

$$\mathrm{grafting\ efficiency(\%)} = \frac{\text{mole of PSSEt linked to natural rubber}}{\text{mole of PSSEt produced during graft copolymerization}} \times 100 \quad (4)$$

where I is the intensity of the signals and the subscript numbers represent the chemical shift (ppm). Table 1 shows

https://doi.org/10.1021/acsomega.4c11363
ACS Omega 2025, 10, 17576−17583

Table 1. DRC Dependence of Conversion and Grafting Efficiency of SSEt[a]

run	DRC (w/w%)	conversion (%)	grafting efficiency (%)
1	15	91	11
2	20	99	20
3	30	coagulation	

[a]Initiator: 3.3×10^{-2} mol/kg-rubber, SSEt: 1.0 mol/kg-rubber.

the DRC dependence of the conversion and grafting efficiency of SSEt at the initiator of 3.3×10^{-2} mol/kg-rubber and SSEt of 1.0 mol/kg-rubber. The conversion and grafting efficiency of SSEt were 99 and 20%, respectively, when the graft copolymerization of SSEt was conducted in latex with a DRC of 20% (Table 1, run 2). These values were higher than those obtained when the DCR of the latex was 15% (w/w) (Table 1, run 1). In contrast, the latex was coagulated when the graft copolymerization was conducted in the latex with a DRC of 30 w/w% (Table 1, run 3). Thus, the suitable DRC of the latex was determined to be 20 w/w%.

Table 2 shows the initiator-concentration dependence of the conversion and grafting efficiency of SSEt at a DRC of 20 w/w

Table 2. Initiator-Concentration Dependence of Conversion and Grafting Efficiency of SSEt[a]

run	initiator concentration (mol/kg-rubber)	conversion (%)	grafting efficiency (%)
1	3.3×10^{-2}	99	20
2	2.0×10^{-2}	98	39
3	1.0×10^{-2}	85	28

[a]DRC: 20 w/w%, SSEt: 1.0 mol/kg-rubber.

% and SSEt of 1.0 mol/kg-rubber. The SSEt conversion was 99% when the graft copolymerization of SSEt was performed with an initiator concentration of 3.3×10^{-2} mol/kg-rubber (Table 2, run 1) and 98% when the initiator concentration was 2.0×10^{-2} mol/kg-rubber (Table 2, run 2). In contrast, the SSEt conversion decreased to 85% for an initiator concentration of 1.0×10^{-2} mol/kg-rubber (Table 2, run 3). This decrease in the SSEt conversion may be due to the reduced amount of initiator generating an insufficient number of radicals to polymerize SSEt. The grafting efficiency of SSEt was the highest (39%; Table 2, run 2) when the graft copolymerization was performed with the initiator of 2.0×10^{-2} mol/kg-rubber, but it decreased to 28 and 20% for an initiator concentration of 1.0×10^{-2} mol/kg-rubber (Table 2, run 3) and 3.3×10^{-2} mol/kg-rubber (Table 2, run 1), respectively. In the graft copolymerization of SSEt onto the surface of the natural rubber particles, radicals as the active sites are generated on the surface of the particles by the addition of the radical initiator into the latex. Then, the propagating polymer radicals generated by the emulsion polymerization of SSEt interact with the radicals on the surface of the natural rubber particles to form a graft copolymer. When the graft copolymerization of SSEt is conducted at excessive initiator concentration, the plural radicals may transfer into a micelle including a propagating polymer radical, after which the radicals may react with each other to form a homopolymer. Thus, the grafting efficiency of SSEt at the initiator of 3.3×10^{-2} mol/kg-rubber was lower. Meanwhile, at a low initiator concentration, the number of radicals generated on the surface of the rubber particles decreases, causing a decrease in the grafting efficiency. This phenomenon is similar to that reported in our previous study for the graft copolymerization of styrene onto the natural rubber particles.[29] Thus, the optimal initiator concentration was determined to be 2.0×10^{-2} mol/kg-rubber.

Table 3 shows the monomer-concentration dependence of conversion and grafting efficiency of SSEt at an initiator of 2.0

Table 3. Monomer-Concentration Dependence of Conversion and Grafting Efficiency[a]

run	monomer concentration (mol/kg-rubber)	conversion (%)	grafting efficiency (%)
1	1.5	coagulation	
2	1.0	98	39
3	0.75	95	43
4	0.50	97	52

[a]DRC: 20 w/w%, initiator: 2.0×10^{-2} mol/kg-rubber.

$\times 10^{-2}$ mol/kg-rubber and a DRC of 20 w/w%. The latex was coagulated when SSEt of 1.5 mol/kg of rubber was graft-copolymerized onto the rubber particles in the latex with a DRC of 20 w/w% (Table 3, run 1). In contrast, the graft copolymerization of SSEt proceeded without coagulation of the latex when its concentration was 1.0, 0.75, and 0.50 mol/kg-rubber, reaching a SSEt conversion of more than 95% (Table 3, runs 2−4). The grafting efficiency of SSEt increased with decreasing SSEt concentration, that is, 39% for the graft copolymerization of SSEt of 1.0 mol/kg-rubber (Table 3, run 2), 43% for 0.75 mol/kg-rubber (Table 3, run 3), and 52% for 0.50 mol/kg-rubber (Table 3, run 4). According to these results, DPNR-*graft*-PSSEt was prepared via graft copolymerization of 1.0, 0.75, and 0.50 mol/kg-rubber of SSEt with an initiator concentration of 2.0×10^{-2} mol/kg-rubber and a DRC of 20 w/w%.

The sulfonic acid ester of the resulting DPNR-*graft*-PSSEt was converted to sulfonic acid via hydrolysis with NaOH as a base catalyst to prevent cyclization of natural rubber, which occurs as a side reaction in the presence of an acid catalyst.[25,26] Figure 3 shows the ^{1}H NMR spectra of DPNR-*graft*-PSSEt prepared with SSEt of 1.0 mol/kg-rubber and DPNR-*graft*-PSS obtained after hydrolysis of DPNR-*graft*-PSSEt with NaOH at 70, 85, and 100 °C. The spectrum of DPNR-*graft*-PSSEt displayed broad signals at 4.1 and 6.8−8.0 ppm, which were assigned to the methylene group of the ethyl ester and the phenyl group of PSSEt, respectively, in addition to the characteristic signals of the *cis*-1,4-isoprene units at 1.8, 2.1, and 5.1 ppm (Figure 3a). In the spectrum of DPNR-*graft*-PSS prepared at 70 °C, new broad signals due to the phenyl group of PSS appeared at 6.6 and 7.6 ppm, and the signals characteristic of PSSEt were still observed at 4.1, 6.9, and 7.8 ppm (Figure 3b). The spectra of DPNR-*graft*-PSS prepared at 85 and 100 °C showed broad signals characteristic of PSS at 6.6 and 7.6 ppm, whereas the characteristic signals of PSSEt completely disappeared (Figure 3c,d). These results demonstrate the successful preparation of DPNR-*graft*-PSS via graft copolymerization of SSEt onto natural rubber particles in the latex stage, followed by hydrolysis with NaOH at 85 and 100 °C.

Characterization of DPNR-*graft*-PSS. Figure 4 shows TEM images of DPNR-*graft*-PSS(1.0), DPNR-*graft*-PSS-(0.75), and DPNR-*graft*-PSS(0.50), which were prepared via graft copolymerization of SSEt at concentrations of 1.0, 0.75,

https://doi.org/10.1021/acsomega.4c11363
ACS Omega 2025, 10, 17576−17583

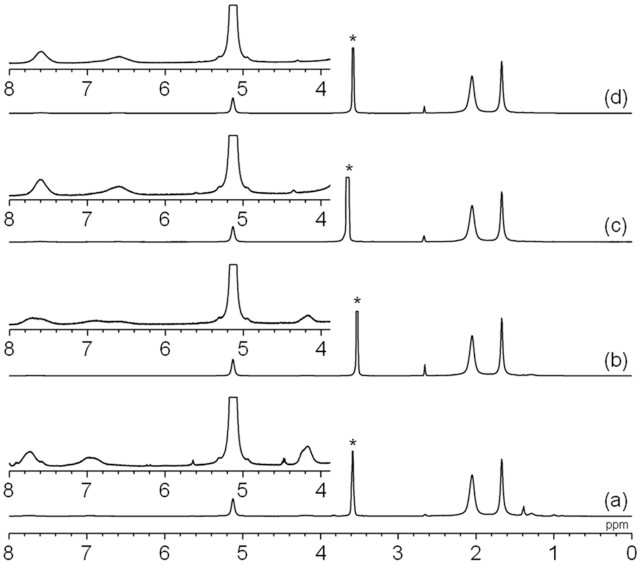

Figure 3. ^{1}H NMR spectra of (a) DPNR-*graft*-PSSEt and DPNR-*graft*-PSS hydrolyzed at (b) 70 °C, (c) 85 °C, and (d) 100 °C. *H_2O in DMSO-d_6.

and 0.50 mol/kg-rubber, respectively, onto natural rubber particles in the latex stage, followed by hydrolysis with NaOH at 85 °C. In these copolymers, the PSS contents were calculated to be 6.5, 5.3, and 4.4%, respectively, from the conversion and the grafting efficiency of SSEt. The bright domains represent DPNR, and the gloomy domains represent PSS owing to staining of the ultrathin sections of DPNR-*graft*-PSS with RuO_4. As shown in Figure 4a, the nanomatrix channel of DPNR-*graft*-PSS(1.0) was formed in which the natural rubber particles with a diameter of approximately 1 μm were covered with a continuous nanochannel of PSS with a thickness of approximately 10 nm. In contrast, the nanochannel of DPNR-*graft*-PSS(0.75) was partially disconnected (Figure 4b). As shown in Figure 4c, for DPNR-*graft*-PSS(0.50), some lumps of PSS with a diameter of about 50−100 nm existed on the surface of the natural rubber particles, forming a discontinuous nanochannel. These differences in the morphology may be attributed to the difference in the PSS content, with the PPS contents of 5.3 and 4.4% in DPNR-*graft*-PSS(0.75) and DPNR-*graft*-PSS(0.50), respectively, being insufficient to form a continuous nanochannel.

Table 4 shows the IEC and σ measured at 50 °C for DPNR, DPNR-*graft*-PSSEt prepared with SSEt of 1.0 mol/kg-rubber, DPNR-*graft*-PSS(1.0), DPNR-*graft*-PSS(0.75), DPNR-*graft*-PSS(0.50), and Nafion117. The IEC and σ of DPNR were 0.00 meq/g and 0.0 S/cm, respectively, owing to the lack of a sulfonic acid group. Meanwhile, the corresponding values for DPNR-*graft*-PSSEt were 0.02 mequiv/g and 1.9×10^{-7} S/cm, suggesting that the hydrolysis of ethyl sulfonate in DPNR-*graft*-PSSEt slightly proceeded by immersing it into 1 mol/L HCl solution followed by drying before the measurement. In contrast, the IEC and σ of DPNR-*graft*-PSS depended significantly on the PSS content. Specifically, the IEC increased from 0.11 to 0.15 and then to 0.22 mequiv/g with increasing PSS content in DPNR-*graft*-PSS(0.50), DPNR-*graft*-PSS-(0.75), and DPNR-*graft*-PSS(1.0), respectively. The IEC of DPNR-*graft*-PSS(1.0) was about one-fourth that of Nafion117 (0.87 meq/g). Similarly, the σ of DPNR-*graft*-PSS increased with increasing PSS content, reaching the highest value of 8.1×10^{-3} S/cm for DPNR-*graft*-PSS(1.0), but it was still lower than that of Nafion117 (4.6×10^{-2} S/cm).

The efficiency of the proton transportation was investigated by estimating the proton conductivity per unit equivalent of sulfonic acid (σ^*) from the values of IEC and σ using the following equation:

$$\sigma^*((\mathrm{S/cm})/\mathrm{meq}) = \frac{\sigma}{\mathrm{IEC}tAd} \quad (5)$$

where t, A, and d are the thickness, surface area, and density of DPNR-*graft*-PSS, respectively. The estimated σ^* values are shown in Table 4. The σ^*s of DPNR and DPNR-*graft*-PSSEt were very low, that is, 0 and 2.8×10^{-4} (S/cm)/meq, respectively. In contrast, the σ^* of DPNR-*graft*-PSS increased with increasing PSS content, showing values of 0.015, 0.50, and 2.6 (S/cm)/meq for DPNR-*graft*-PSS(0.50), DPNR-*graft*-PSS(0.75), and DPNR-*graft*-PSS(1.0), respectively. Furthermore, the σ^* of DPNR-*graft*-PSS(1.0) was approximately 1.4 times higher than that of Nafion117, (1.9 (S/cm)/meq), which can be attributed to the formation of a continuous nanochannel of PSS, as shown in Figure 4a.

Figure 5 shows the Arrhenius plot of σ versus $1/T$ for DPNR-*graft*-PSSEt, DPNR-*graft*-PSS, and Nafion117. The σ values for all specimens depended on the temperature, showing higher values with increasing temperature. The apparent activation energies of DPNR-*graft*-PSSEt, DPNR-*graft*-PSS, and Nafion117 were estimated from the slope of the plots (Table 5). The apparent activation energy of DPNR-*graft*-PSSEt was 103.6 kJ/mol, whereas those of DPNR-*graft*-PSS(1.0), DPNR-*graft*-PSS(0.75), and DPNR-*graft*-PSS(0.50) were remarkably lower, that is, 3.2, 2.7, and 1.5 kJ/mol, respectively. These values were lower than those of Nafion117 (13.0 kJ/mol), which suggests that the proton transportation occurs more efficiently in DPNR-*graft*-PSS than in Nafion117.

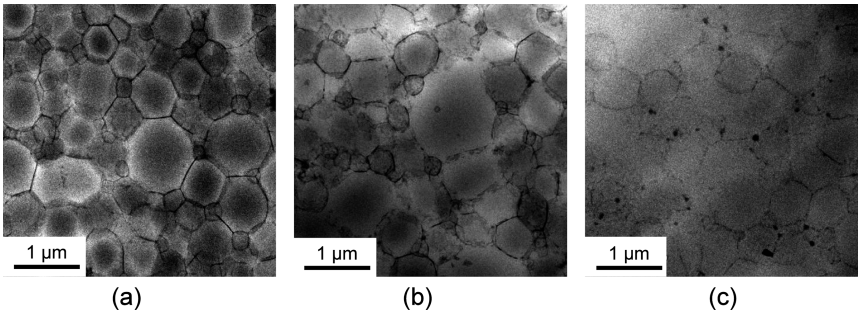

Figure 4. TEM images of (a) DPNR-*graft*-PSS(1.0), (b) DPNR-*graft*-PSS(0.75), and (c) DPNR-*graft*-PSS(0.50).

https://doi.org/10.1021/acsomega.4c11363
ACS Omega 2025, 10, 17576−17583

Table 4. Proton Conductivity and IEC of DPNR, DPNR-*graft*-PSSEt, DPNR-*graft*-PSS, and Nafion117

specimen	SSEt-concentration (mol/kg-rubber)	thickness (mm)	IEC (meq/g)	conductivity, σ (S/cm)[a]	conductivity per unit equivalent of sulfonic acid, σ^* ((S/cm)/meq)
DPNR		0.399	0.00	0.0	0.0
DPNR-*graft*-PSSEt	1.0	0.481	0.02	1.9×10^{-7}	2.8×10^{-4}
DPNR-*graft*-PSS(0.50)	0.50	0.277	0.11	3.2×10^{-5}	0.015
DPNR-*graft*-PSS(0.75)	0.75	0.205	0.15	1.4×10^{-3}	0.50
DPNR-*graft*-PSS(1.0)	1.0	0.204	0.22	8.1×10^{-3}	2.6
Nafion117		0.185	0.87	4.6×10^{-2}	1.9

[a]Measured at 50 °C.

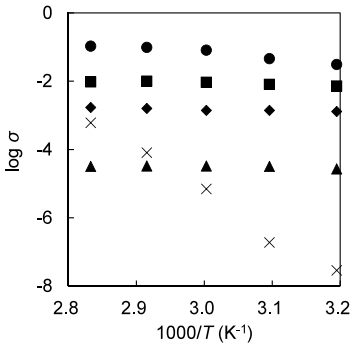

Figure 5. Arrhenius plot for proton conductivity, σ, of DPNR-*graft*-PSSEt (×), DPNR-*graft*-PSS(1.0) (box solid), DPNR-*graft*-PSS-(0.75) (tilted square solid), DPNR-*graft*-PSS(0.50) (triangle up solid), and Nafion117 (circle solid).

Table 5. Apparent Activation Energy Estimated from the Slope of Arrhenius Plot

specimen	SSEt-concentration (mol/kg-rubber)	activation energy (kJ/mol)
DPNR-*graft*-PSSEt	1.0	103.6
DPNR-*graft*-PSS(0.50)	0.50	1.5
DPNR-*graft*-PSS(0.75)	0.75	2.7
DPNR-*graft*-PSS(1.0)	1.0	3.2
Nafion117		13.0

Proton transportation can proceed via two mechanisms, that is, Grotthuss and vehicle mechanisms.[30] In the vehicle mechanism, proton transport occurs via diffusion as the hydrated proton. In contrast, in the Grotthuss mechanism, protons are transported by jumping from one sulfonic acid molecule to another. The two mechanisms can be well distinguished from each other according to the apparent activation energy, that is, the apparent activation energy of the vehicle mechanism is higher than 20 kJ/mol, whereas that of the Grotthuss mechanism is usually lower than 15 kJ/mol.[31] Thus, the proton transportation in DPNR-*graft*-PSS and Nafion 117 most likely occurs via the Grotthuss mechanism, whereas that in DPNR-*graft*-PSSEt proceeds via the vehicle mechanism. The difference in the mechanism between DPNR-*graft*-PSS and DPNR-*graft*-PSSEt can be attributed to the content of the sulfonic acid groups. In DPNR-*graft*-PSS, the large amount of sulfonic acid groups in the nanochannel of PSS with a thickness of approximately 10 nm facilitates proton jumping. In contrast, owing to the lower amount of sulfonic acid groups in DPNR-*graft*-PSSEt, protons are transported via diffusion of hydrated protons. These results demonstrate that the PEM with a nanomatrix channel consisting of natural rubber and PSS achieved efficient proton transportation via the Grotthuss mechanism.

Figure 6 shows the stress−strain curves for DPNR and DPNR-*graft*-PSS. For DPNR-*graft*-PSS, the stress at 100% strain increased with increasing PSS content, showing values of 0.6 MPa for DPNR-*graft*-PSS(1.0), 0.3 MPa for DPNR-*graft*-PSS(0.75), and 0.1 MPa for DPNR-*graft*-PSS(0.50). Meanwhile, the stress at 100% strain of DPNR was 0.2 MPa. The values of stress and strain at break of DPNR were 3.4 MPa and 870%, respectively. For DPNR-*graft*-PSS(1.0) and DPNR-*graft*-PSS(0.75), the stress increased abruptly at a strain of approximately 400%, reaching 6.9 MPa at break, and the strain at break was similar to that of DPNR, that is, 790 and 880%, respectively. In our previous studies,[32,33] the nanomatrix structure consisting of natural rubber particles with a diameter of approximately 1 μm covered with a continuous phase of polystyrene with a thickness of about 15 nm was found to increase the stress at break of the graft copolymer. Thus, the high stress at break of DPNR-*graft*-PSS(1.0) and DPNR-*graft*-PSS(0.75) can be attributed to the continuous nanomatrix channel consisting of natural rubber and PSS. However, the stress at break of DPNR-*graft*-PSS(0.50) was lower than that of DPNR. The low stress at 100% strain and at break of DPNR-*graft*-PSS(0.50) may be due to its lower PPS content. According to these results, the nanomatrix channel consisting of natural rubber and a continuous nanochannel of PSS improved not only the proton conductivity but also the tensile strength. In particular, DPNR-*graft*-PSS(1.0) was proved to be a rubbery soft PEM with outstanding proton conductivity.

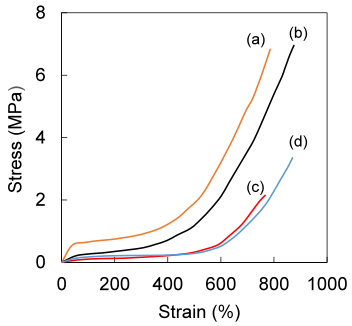

Figure 6. Stress−strain curves of (a) DPNR-*graft*-PSS(1.0), (b) DPNR-*graft*-PSS(0.75), (c) DPNR-*graft*-PSS(0.50), and (d) DPNR.

https://doi.org/10.1021/acsomega.4c11363
ACS Omega 2025, 10, 17576−17583

CONCLUSIONS

A rubbery soft PEM with a nanomatrix channel consisting of natural rubber and a continuous nanochannel of PSS was prepared via graft copolymerization of SSEt onto natural rubber particles in the latex stage, followed by hydrolysis with NaOH. The PSS content of DPNR-*graft*-PSS(1.0), DPNR-*graft*-PSS(0.75), and DPNR-*graft*-PSS(0.50) was 6.5, 5.3, and 4.4%, respectively. TEM observation confirmed the formation of a nanomatrix channel in DPNR-*graft*-PSS(1.0). The IEC and σ values of DPNR-*graft*-PSS increased with increasing PSS content, reaching 0.22 meq/g and 8.1×10^{-3} S/cm, respectively, for DPNR-*graft*-PSS(1.0). Meanwhile, the σ^* value of DPNR-*graft*-PSS(1.0) was 2.6 (S/cm)/meq, which was higher than that of Nafion117. The apparent activation energy for the proton conductivity was 3.2 kJ/mol for DPNR-*graft*-PSS(1.0), 2.7 kJ/mol for DPNR-*graft*-PSS(0.75), and 1.5 kJ/mol for DPNR-*graft*-PSS(0.50), suggesting that proton transportation occurred via the Grotthuss mechanism. The stress at break of DPNR-*graft*-PSS(1.0) was 6.9 MPa, which was about twice that of DPNR. Thus, DPNR-*graft*-PSS(1.0) exhibited superior σ^*, apparent activation energy of proton conductivity, and tensile strength, which can be attributed to the nanomatrix channel promoting the effective transportation of protons and improving the tensile strength.

ASSOCIATED CONTENT

Supporting Information

The Supporting Information is available free of charge at https://pubs.acs.org/doi/10.1021/acsomega.4c11363.

Procedure of preparation of *p*-styrenesulfonic acid (SS), procedure of graft copolymerization of SS or SSNa onto natural rubber particles, ^{1}H NMR spectra of DPNR-*graft*-PSS prepared by graft copolymerization of SS, ^{1}H NMR spectra DPNR-*graft*-PSSNa prepared by graft copolymerization of SSNa, and stress−strain curves of DPNR and DPNR-*graft*-PSS (PDF)

AUTHOR INFORMATION

Corresponding Author

Yoshimasa Yamamoto − *Department of Chemical Science and Engineering, National Institute of Technology, Tokyo College, Hachioji, Tokyo 193-0997, Japan;* orcid.org/0000-0002-8326-8840; Email: yamamoto@tokyo-ct.ac.jp

Author

Seiichi Kawahara − *Department of Materials Science and Bioengineering, Nagaoka University of Technology, Nagaoka, Niigata 940-2188, Japan;* orcid.org/0000-0002-6702-6497

Complete contact information is available at: https://pubs.acs.org/10.1021/acsomega.4c11363

Author Contributions

Y.Y. performed the preparation of specimens, observation of morphology, measurement of proton conductivity and wrote the manuscript. S.K. contributed to the characterization of the specimens with NMR and provided scientific support. All authors contributed to the manuscript. All authors have given approval to the final version of the manuscript.

Notes

The authors declare no competing financial interest.

ACKNOWLEDGMENTS

This work was supported in part by a grant-in-aid (22K05234) for Scientific Research (C) from Japan Society for the Promotion of Science.

REFERENCES

(1) Kawahara, S.; Suksawad, P.; Yamamoto, Y.; Kuroda, H. Nanomatrix Channel for Ionic Molecular Transportation. *Macromolecules* **2009**, *42*, 8557−8560.

(2) Suksawad, P.; Kosugi, K.; Yamamoto, Y.; Akabori, K.; Kuroda, H.; Kawahara, S. Polymer Electrolyte Membrane with Nanomatrix Channel Prepared by Sulfonation of Natural Rubber Grafted with Polystyrene. *J. Appl. Polym. Sci.* **2011**, *122*, 2403−2414.

(3) Fukuhara, L.; Kado, N.; Kosugi, K.; Suksawad, P.; Yamamoto, Y.; Ishii, H.; Kawahara, S. Preparation of Polymer Electrolyte Membrane with Nanomatrix Channel Through Sulfonation of Natural Rubber Grafted with Polystyrene. *Solid State Ionics* **2014**, *268*, 191−197.

(4) Nawamawat, K.; Sakdapipanich, J. T.; Ho, C. C.; Ma, Y.; Song, J.; Vancso, J. G. Surface Nanostructure of *Hevea brasiliensis* Natural Rubber Latex Particles. *Colloids Surf., A* **2011**, *390*, 157−166.

(5) Tanaka, Y. Structural Characterization of Natural Polyisoprenes: Solve the Mystery of Natural Rubber. *Rubber Chem. Technol.* **2001**, *74*, 355−375.

(6) Weber, A. Z.; Newman, J. Modeling Transport in Polymer-Electrolyte Fuel Cells. *Chem. Rev.* **2004**, *104*, 4679−4726.

(7) Meng, H.; Song, J.; Guan, P.; Wang, H.; Zhao, W.; Zou, Y.; Ding, H.; Wu, X.; He, P.; Liu, F.; Zhang, Y. High Ion Exchange Capacity Perfluorosulfonic Acid Resine Proton Exchange Membrane for High Temperature Applications in Polymer Electrolyte Fuel Cells. *J. Power Sources* **2024**, *602*, No. 234205.

(8) Hu, C.; Deng, X.; Dong, X.; Hong, Y.; Zhang, Q.; Liu, Q. Rigid Crosslinkers Towards Constructing Highly-efficient Ion Transport Channels in Anion Exchange Membranes. *J. Membr. Sci.* **2021**, *619*, No. 118806.

(9) Vishnyakov, A.; Neimark, A. V. Molecular Dynamics Simulation of Microstructure and Molecular Mobilities in Swollen Nafion Membranes. *J. Phys. Chem. B* **2001**, *105*, 9586−9594.

(10) Karimi, M. B.; Mohammadi, F.; Hooshyari, K. Recent Approaches to Improve Nafion Performance for Fuel Cell Applications: A Review. *Int. J. Hydrog. Energy* **2019**, *44*, 28919−28938.

(11) Evich, M. G.; Davis, M. J. B.; McCord, J. P.; Acrey, B.; Awkerman, J. A.; Knappe, D. R. U.; Lindstrom, A. B.; Speth, T. F.; Tebes-Stevens, C.; Strynar, M. J.; Wang, Z.; Weber, E. J.; Henderson, W. M.; Washington, J. W. Per- and Polyfluoroalkyl Substances in the Environment. *Science* **2022**, *375*, No. eabg9065.

(12) Interial, L. G. D.; Benavides, R.; Morales-Acosta, D.; Francisco-Vieira, L.; Da Silva, L. Development of Polymeric Electrolytes for Fuel Cells: Synthesis and Characterization of New Sulfonated Polystyrene-co-Acrylonitrile-co-Butyl Acrylate Terpolymers. *Solid State Ionics* **2022**, *387*, No. 116066.

(13) Smitha, B.; Sridhar, S.; Khan, A. A. Synthesis and Characterization of Proton Conducting Polymer Membranes for Fuel Cells. *J. Membr. Sci.* **2003**, *225*, 63−76.

(14) Mahimai, B. M.; Sivasubramanian, G.; Sekar, K.; Kannaiyan, D.; Deivanayagam, P. Sulfonated Poly(ether ether ketone): Efficient Ion-exchange Polymer Electrolytes for Fuel Cell Applications−A Versatile Review. *Mater. Adv.* **2022**, *3*, 6085−6095.

(15) Pokprasert, A.; Theato, P.; Chirachanchai, S. Proton Donor/Acceptor Copolymer Brushes on Sulfonated Poly(ether ether ketone) Membrane: An Approach to Construct Efficient Proton Transfer Pathway in Polymer Electrolyte Membrane Fuel Cell. *Polymer* **2022**, *240*, No. 124523.

(16) Yoshida-Hirahara, M.; Takahashi, S.; Yoshizawa-Fujita, M.; Takeoka, Y.; Rikukawa, M. Synthesis and Investigation of Sulfonated Poly(p-phenylene)-Based Ionomers with Precisely Controlled Ion Exchange Capacity for Use as Polymer Electrolyte Membranes. *RSC Adv.* **2020**, *10*, 12810−12822.

(17) Zhang, J.; Zhu, C.; Xu, J.; Wu, J.; Yin, X.; Chen, S.; Zhu, Z.; Wang, L.; Li, Z.-C. Enhanced Mechanical Behavior and Electrochemical Performance of Composite Separator by Constructing Crosslinked Polymer Electrolyte Networks on Polyphenylene Sulfide Nonwoven Surface. *J. Membr. Sci.* **2020**, *597*, No. 117622.
(18) Aili, D.; Kraglund, M. R.; Tavacoli, J.; Chatzichristodoulou, C.; Jensen, J. O. Polysulfone-Polyvinylpyrrolidone Blend Membranes as Electrolytes in Alkaline Water Electrolysis. *J. Membr. Sci.* **2020**, *598*, No. 117674.
(19) Ryu, G. Y.; An, S. J.; Yu, S.; Kim, K. J.; Jae, H.; Roh, D.; Chi, W. S. Dual-Sulfonated MOF/Polysulfone Composite Membranes Boosting Performance for Proton Exchange Membrane Fuel Cells. *Eur. Polym. J.* **2022**, *180*, No. 111601.
(20) Hooshyari, K.; Rezania, H.; Vatanpour, V.; Salarizadeh, P.; Askari, M. B.; Beydaghi, H.; Enhessari, M. High Temperature Membranes Based on PBI/Sulfonated Polyimide and Doped-Perovskite Nanoparticles for PEM Fuel Cells. *J. Membr. Sci.* **2020**, *612*, No. 118436.
(21) He, Z.; Wang, G.; Wei, S.; Li, G.; Zhang, J.; Chen, J.; Wang, R. A Novel Fluorinated Acid-Base Sulfonated Polyimide Membrane with Sulfoalkyl Side-Chain for Vanadium Redox Flow Battery. *Electrochim. Acta* **2021**, *399*, No. 139434.
(22) Sato, K.; Kajita, T.; Noro, A. Synthesis of a Cross-Linked Polymer Electrolyte Membrane with an Ultra-High Density of Sulfonic Acid Groups. *ACS Appl. Polym. Mater.* **2023**, *5*, 3480−3488.
(23) Chen, L.; Hallinan, D. T., Jr; Elabd, Y. A.; Hillmyer, M. A. Highly Selective Polymer Electrolyte Membranes from Reactive Block Polymers. *Macromolecures* **2009**, *42*, 6075−6085.
(24) Kawahara, S.; Kawazura, T.; Sawada, T.; Isono, Y. Preparation and Characterization of Natural Rubber Dispersed in Nano-matrix. *Polymer* **2003**, *44*, 4527−4531.
(25) Riyajan, S.; Tanaka, Y.; Sakdapipanich, J. T. Preparation of Cyclized Deproteinized Natural Rubber in Latex State via a Combination of Benzotrichloride and Sulfuric Acid System, and Its Properties. *Rubber Chem. Technol.* **2007**, *80*, 365−377.
(26) Lee, D. F.; Scanlan, J.; Watson, W. F. The Cyclization of Natural Rubber. *Rubber Chem. Technol.* **1963**, *36*, 1005−1018.
(27) Zeng, G.; Zhang, D.; Yan, L.; Yue, B.; Pan, T.; Hu, Y.; He, S.; Zhao, H.; Zhang, J. Design and Synthesis of Side-Chain Optimized Poly(2,6-dimethyl-1,4-phenylene oxide)-*g*-Poly(styrene sulfonic acid) as Proton Exchange Membrane for Fuel Cell Applications: Balancing the Water-Resistance and the Sulfonation Degree. *Int. J. Hydrog. Energy* **2021**, *46*, 20664−20677.
(28) Fukushima, Y.; Kawahara, S.; Tanaka, Y. Synthesis of Graft Copolymer from Highly Deproteinized Natural Rubber. *J. Rubber Res.* **1998**, *1*, 154−166.
(29) Pukkate, N.; Yamamoto, Y.; Kawahara, S. Mechanism of graft copolymerization of styrene onto deproteinized natural rubber. *Colloid Polym. Sci.* **2008**, *286*, 411−416.
(30) Saito, M.; Hayamizu, K.; Okada, T. Temperature Dependence of Ion and Water Transport in Perfluorinated Ionomer Membranes for Fuel Cells. *J. Phys. Chem. B* **2005**, *109*, 3112−3119.
(31) Wu, H.; Cai, H.; Xu, Y.; Wu, Q.; Yan, W. Hybrid Electrolyte SiW_9MoV_2/rGO/SPEEK for Solid Supercapacitors with Enhanced Conductive Performance. *Mater. Chem. Phys.* **2018**, *215*, 163−167.
(32) Kawahara, S.; Yamamoto, Y.; Fujii, S.; Isono, Y.; Niihara, K.; Jinnai, H.; Nishioka, H.; Takaoka, A. FIB-SEM and TEMT Observation of Highly Elastic Rubbery Material with Nanomatrix Structure. *Macromolecules* **2008**, *41*, 4510−4513.
(33) Yamamoto, Y.; Endo, K.; Tévenot, Q.; Kosugi, K.; Nakajima, K.; Kawahara, S. Entropic and Energetic Elasticities of Natural Rubber with a Nanomatrix Structure. *Langmuir* **2020**, *36*, 11341−11348.

https://doi.org/10.1021/acsomega.4c11363
ACS Omega 2025, 10, 17576−17583